Integrated Solar Geometry Modelling and Real-Time Environmental Monitoring for Photovoltaic Performance Optimisation

Halah Al-Saadi *‡, Ahmed Jabbar Abid *, Adel Ahmed Obed *

* Department of Electrical Engineering Techniques, Electrical Engineering Technical College, Middle Technical University, Baghdad, Iraq

(bcc4012@mtu.edu.iq, dr.ahmedjabbar@mtu.edu.iq, adelrazan@mtu.edu.iq)

‡Corresponding Author; Halah Al-Saadi, Department of Electrical Engineering Techniques, Electrical Engineering Technical College, Middle Technical University, Baghdad, Iraq, bcc4012@mtu.edu.iq

Received: 12.08.2025 Accepted:08.09.2025

Abstract- Photovoltaic (PV) systems are important for advancing renewable energy generation; however, their operational efficiency is strongly dependent on fluctuating environmental conditions. Variations in solar irradiance, ambient temperature, wind speed, and angle of incidence interact to influence PV cell temperature and, consequently, power output. While these factors have been examined individually in previous studies, integrated approaches that combine continuous environmental monitoring with real-time performance modelling remain limited. This study presents a year-long analysis in which theoretical solar geometry calculations were coupled with high-resolution empirical measurements. Solar position parameters were derived dynamically, enabling real-time cell temperature and efficiency estimation. The results show that efficiency decreased from the nominal 15% under standard test conditions to an average of 13.0% under field conditions, reflecting the effect of elevated temperatures and variable irradiance. Wind speed provided a measurable cooling effect, reducing cell temperature by up to 12 °C at 15–17 m/s and thereby mitigating thermal losses. Furthermore, variations in the angle of incidence were identified as a key factor driving short-term efficiency fluctuations. Validation of the predictive efficiency model (Eq. 11) against measured data demonstrated strong consistency (deviations < 8%). These findings underscore the importance of incorporating adaptive orientation mechanisms and effective thermal management strategies into PV system design. The integrated modelling–measurement approach proposed here offers a more accurate basis for site-specific performance prediction and system optimisation.

Keywords: Environmental monitoring, solar incident angle, photovoltaic system performance, wind measurement, thermal analysis.

1. Introduction

Rapid population growth, coupled with accelerated technological development, has driven a substantial rise in global energy demand, with consumption rising by 69% between 1990 and 2020, driven by a 48% population growth and expanding industrial sectors [1, 2]. Projections estimate a further increase in energy demand by 9% to 53% by 2050 under various scenarios [3]. Given fossil fuels' finite nature and environmental impact, there is an urgent shift toward renewable energy sources, particularly in electricity generation [4].

Renewables contributed 30.7% of global electricity in 2023, with solar alone expected to generate up to 18,000 TWh by 2050 [3, 5]. Solar photovoltaics (PV), favoured for their scalability and low emissions, have seen rapid adoption, surpassing thermal systems with 672 GW installed by 2019 and reaching 1,182 GW by 2023 [6], [7]. However, increasing deployment alone does not guarantee consistent energy yield.

The actual power delivered by PV systems depends strongly on site-specific environmental conditions, including irradiance, ambient temperature, wind velocity, and the incidence angle of sunlight. Understanding and addressing

these dependencies is therefore critical for maximising the value of PV within the renewable energy mix. Nevertheless, the operational efficiency of PV systems is strongly influenced by environmental conditions such as solar irradiance, cell temperature, wind velocity, ambient humidity, and the incidence angle of sunlight on the module surface [8-11]. Notably, cell temperature can decrease power output by 0.3–0.5% per °C increase [12-14], and optimal panel inclination and solar incidence angles are significant for maximising efficiency [15-18].

Earlier studies have established that photovoltaic cell temperature and conversion efficiency are markedly affected by environmental variables, including solar irradiance, ambient temperature, and wind speed [19-22]. Traditional PV monitoring methods, reliant on manual logging or fixed-location stations, lack the resolution and adaptability needed for real-time performance evaluation [23]. To overcome this limitation, this study presents a novel, autonomous monitoring system capable of real-time measurement of solar irradiance, ambient and cell temperature, wind speed, and incidence angle, with integrated efficiency computation—operating independently without external power or data systems.

The proposed system demonstrates strong correlations between environmental conditions and PV efficiency, offering a practical solution for field deployment and long-term performance diagnostics. This work uniquely contributes by integrating all critical PV performance parameters into a standalone, self-powered device, enabling continuous monitoring and optimisation of PV systems in diverse climatic conditions.

Unlike prior works that examined irradiance, temperature, and wind speed separately, this study introduces an integrated monitoring–modelling approach. By combining solar geometry calculations with real-time environmental measurements, we provide a unified framework for predicting PV efficiency. This foundation enables future optimisation using multivariate and machine learning methods. To ensure the reliability of the proposed solar monitoring system, a validation study was conducted, as detailed in Section 3.

2. Methodology

2.1. Experimental Framework

This study investigates the influence of environmental factors on PV performance modelling [19], [24], [25]. The monitoring system was built around an Arduino Mega 2560 with integrated sensors, including a pyranometer (irradiance), DS18B20 (ambient and module temperature), and an anemometer (wind speed). A DS3231 RTC provided timestamping [26-28]. A summary of all components and their functions is shown in Table 1

2.2. Experimental Framework

The monitoring system comprises the following principal hardware components (Table 1). The hardware configuration and interconnections are depicted in Figure 1, illustrating the overall system architecture.

Table 1. Hardware components utilised in the PV monitoring system.

Component	Description and Function
Arduino Mega 2560	Central data acquisition and processing unit
DS18B20 Temp. Sensor	Measures ambient air temperature and PV module surface temperature
Anemometer	Measures wind speed (m/s), essential for convective cooling estimation
Pyranometer	Measures global solar irradiance (W/m²)
DS3231 Real-Time Clock	Provides accurate timestamping for synchronised data logging

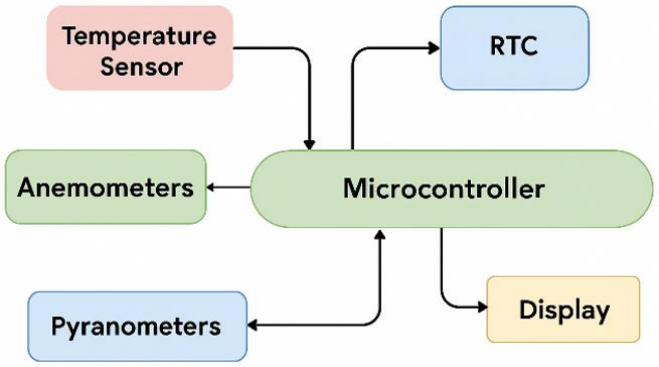

Fig. 1. Block diagram of photovoltaic (PV) performance monitoring system.

2.3. Data Acquisition and Computational Methods

Sensor readings were acquired at predefined intervals and processed in situ via embedded software developed in the Arduino Integrated Development Environment (IDE). Custom algorithms based on validated solar engineering models were implemented to compute solar position parameters, PV cell temperature, and efficiency metrics.

2.4. Solar Position Calculations

Solar position parameters were computed to precisely determine the angle at which incoming radiation strikes the photovoltaic surface. The following equations were employed:

- Apparent Solar Time (AST): Solar time and local clock time differ, depending on the day of the year and the designated time zone. Solar time is utilised to estimate solar energy based on the sun's apparent angular movement across the sky. One method of expressing solar time is:

$$AST = LST + EoT \pm 4(SL - LL) - DS \quad (1)$$

Where, LST represents local standard time, EoT is the equation of time (minutes), SL is standard

longitude, LL is local latitude, and DS denotes daylight saving time adjustment (0 or 60 min).

- Equation of Time:

$$EoT = 9.87\ sin(2B) - 7.53\ cos(B)\ - 1.5\ sin(B) \quad (2a)$$

$$B\ = \left(\frac{360}{365}\right)(N\ -\ 81) \quad (2b)$$

Where B is the angle of the day, and N is the day of the year (from 1 to 365).

- Day of Year (N): from the RTC involves converting the current date (day, month, year) into a sequential day number from 1 to 365 (or 366 in a leap year).
- Declination Angle (δ): The angle created by the Sun's rays and the Earth's equator's plane is called the Declination Angle (δ).

$$\delta\ =\ 23.45\ sin\ [\left(\frac{360}{365}\right)(284\ +\ N)] \quad (3)$$

- Hour Angle (h): The Hour Angle (h) describes the Sun's position relative to solar noon.

$$h\ =\ (\ AST\ -\ 12\ )\ \times 15 \quad (4)$$

- LST: At local solar noon, the apparent solar time (AST) is 12, and the solar altitude (h) is 0º.

$$LST\ =\ 12 - EoT\ \pm\ 4(SL\ -LL) \quad (5)$$

- Sunrise and sunset times and day length: Given that the hour angle at local solar noon is 0°, and each 15° of longitude corresponds to 1 hour.

$$Hss\ = -\ Hsr = \left(\frac{1}{15}\right)\cos^{-1}(-\ tan\ (L) \times tan(\delta)\ ) \quad (6)$$

Where L is the latitude of a location in degrees. When solar noon transpires between sunrise (Hsr) and sunset time (Hss), the day length is double that of the period from solar noon to sunset.

$$Day\ Length = 2\ Hss \quad (7)$$

- Incident angle (θ): The angle formed between the sun's rays and the surface of a photovoltaic panel is:

$$\begin{aligned} &Cos(\theta) \\ &= sin(L)\ sin(\delta)\ cos(\beta) \\ &-\ cos(L)\ sin(\delta)\ sin(\beta)\ cos(Zs) \\ &+\ cos(L)\ cos(\delta)\ cos(h)\ cos(\beta) \\ &+\ sin(L)\ cos(\delta)\ cos(h)\ sin(\beta)\ sin(Zs) \\ &+\ cos(\delta)\ sin(h)\ sin(\beta)\ sin(Zs) \end{aligned} \quad (8)$$

2.5. Solar Position Calculations

Numerous factors can impact how temperature influences the efficiency of a photovoltaic (PV) cell.

$$Tc\ =\ 0.943Ta\ +\ 0.0195G\ -\ 1.528Va\ +\ 273 \quad (9)$$

Where; Tc: PV cell temperature in kelvin (K), Ta: Ambient air temperature in degrees Celsius (°C), G: Solar irradiance in watts per square meter (W/ m^2), Va: Wind speed in meters per second (m\s), and 273.5029: A constant to convert from Celsius to kelvin (since 0°C = 273.15K) [29-32].

2.6. Photovoltaic Efficiency Calculation

The efficiency of the PV panel was corrected for temperature variations according to:

$$\eta = \eta_{stc} \times (\ 1 - \beta\ (T_c - 25)) \quad (10)$$

Where β is the power variation due to temperature. The effective efficiency is calculated based on the cos(θ) which is expressed as:

$$\eta_{Total} = \eta \times cos(\theta) \times 100\% \quad (11)$$

2.7. System Architecture and Implementation

The system's architecture is centred on the Arduino Mega 2560 microcontroller, which acquires sensor inputs, performs real-time data processing, and outputs calculated parameters via an LCD interface. This methodological framework facilitates continuous, autonomous monitoring of PV environmental and performance parameters, enabling detailed analysis of efficiency variations due to meteorological factors over extended periods. The integration of accurate solar geometry computations with real-time sensor data provides a robust platform for evaluating PV system behaviour in situ.

The overall block diagram of the system is presented in Figure 1, while Figure 2 illustrates the physical prototype. The embedded software workflow, summarising sensor polling, computation routines, and data display sequences, is shown in Figure 3.

To validate the accuracy of the efficiency predictions shown in Figure 3, the results were compared with experimental measurements from the Arduino-based monitoring system. The agreement between predicted and measured values was strong, with an average deviation of less than 8%. This confirms the reliability of the proposed model for estimating PV efficiency under varying environmental conditions.

Fig. 2. System prototype.

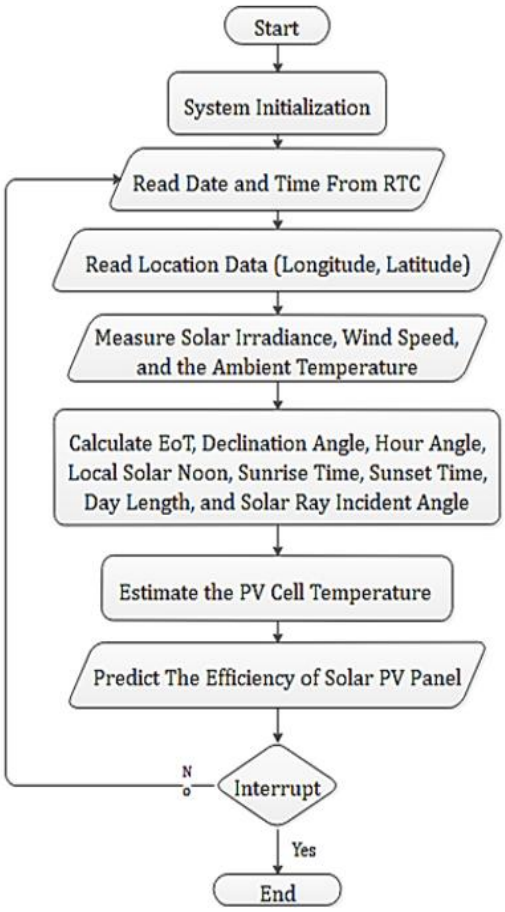

Fig. 3. Software flowchart.

3. Results and Discussion

The performance of photovoltaic (PV) systems was assessed using experimentally simulated datasets acquired through an Arduino-based environmental monitoring suite.

Critical variables—including ambient temperature, solar irradiance, and wind speed—were continuously recorded and incorporated into models quantifying their effects on PV cell temperature and conversion efficiency. Complementary astronomical parameters, such as day length, local solar noon, sunrise and sunset times, and angle of incidence, were also analysed to ensure a comprehensive evaluation. The findings are illustrated through a series of graphical representations and interpreted as follows.

To evaluate the precision of the modelled photovoltaic (PV) system, the calculated efficiency was compared with the standard reference efficiency under Standard Test Conditions (STC), which assumes an irradiance of 1000 W/m² and an ambient temperature of 25 °C. Under STC, the typical efficiency of the PV module is approximately 15%. In contrast, the experimental results obtained from the proposed system yielded an average efficiency of 13.02%, reflecting the influence of elevated ambient temperatures (average 32.2 °C) and variable solar irradiance. This corresponds to approximately 86.8% of the nominal STC performance, demonstrating the realistic behaviour of the proposed model under actual environmental conditions. Under field operation, the average efficiency was 13.02% (0.87×STC). This value is consistent with reported performance-ratio ranges for operating plants (≈0.6–0.9, with ~0.8 typical for newer systems) and aligns with temperature-coefficient expectations of ~–0.4% to –0.5% per °C at elevated operating temperatures [33-35]. To account for measurement reliability, manufacturer-specified error margins were considered: ±5% for irradiance, ±0.5 °C for temperature, and ±0.3 m/s for wind speed. These steps confirm the robustness and accuracy of the proposed model for predicting PV efficiency under real-world conditions.

3.1. System Architecture and Implementation

A sinusoidal variation in day length was observed over the year, with durations ranging from ~9.5 hours in winter (around day 355) to ~14.5 hours in summer (around day 172). This variation results from the Earth's axial tilt and orbit. The data are consistent with astronomical models and provide important boundary conditions for daily solar energy availability and performance optimization, as in Figure 4.

3.2. Annual Variations in Local Solar Noon Timing

The local solar noon exhibited a waveform variation throughout the year, ranging from approximately 11.6 to 12.5 hours. This fluctuation is governed by the Equation of Time (EoT) and the Earth's elliptical orbit. Maxima were noted around day 160 (early June) and day 355 (late December), while minima appeared near days 90 and 250. These variations influence the timing of peak irradiance and must be accounted for in sun-tracking and system optimisation algorithms, as shown in Figure 5.

3.3. Annual Variations in Local Solar Noon Timing

The relationship between ambient temperature and cell temperature was examined at irradiance levels of 600 W/m² and 1000 W/m². In both cases, a linear increase in Tc with increasing Ta was evident. The cell temperature rose from approximately 20 °C to 90 °C as the ambient temperature increased from 0 °C to 60 °C. At Ta = 30 °C, for example, Tc reached ~49 °C for G = 600 W/m² and ~61 °C for G = 1000 W/m².

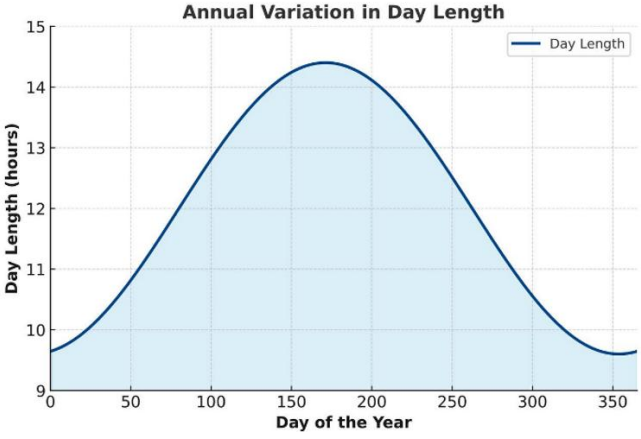

Fig. 4. Annual variation in day length.

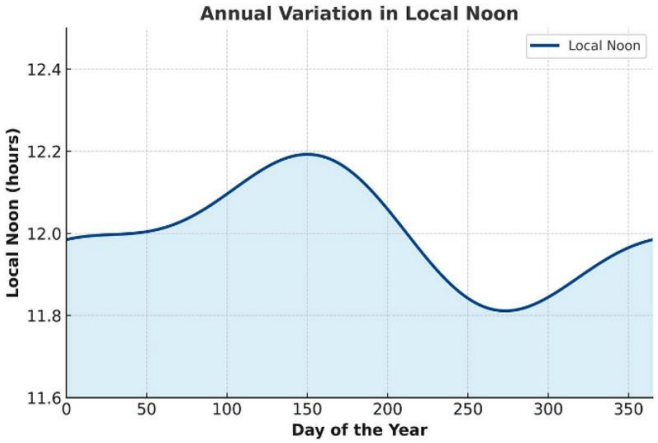

Fig. 5. Annual variation in local noon.

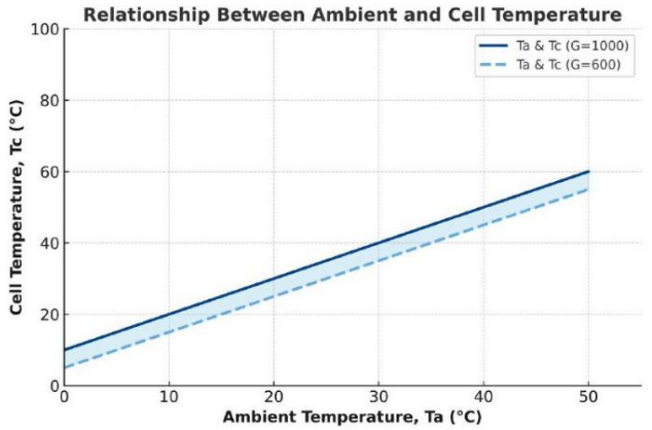

Fig. 6. Relationship between ambient and cell temperature.

This demonstrates that higher irradiance exacerbates the thermal impact of rising ambient temperatures, underscoring the need for thermal management in high-temperature regions, as shown in Figure 6.

3.4. Impact of Solar Irradiance Variations on Photovoltaic Cell Temperature

A proportional linear correlation between solar irradiance (G) and cell temperature (Tc) was observed under two ambient temperature conditions (30 °C and 40 °C). As irradiance increased from 0 to 1000 W/m², the cell temperature rose proportionally in both conditions. For instance, at $G \approx 865\ W/m^2$, Tc reached approximately 42.1 °C when Ta = 30 °C and 51.5 °C when Ta = 40 °C. This confirms that both solar irradiance and ambient temperature contribute cumulatively to cell heating, which is critical for understanding and mitigating efficiency loss in PV systems operating in warm climates, as shown in Figure 7.

3.5. Effect of Wind Velocity on Photovoltaic Cell Temperature

An inverse relationship between wind speed (Va) and cell temperature was observed. As wind speed increased from 0 to ~17 m/s, the PV cell temperature dropped from approximately 55 °C to 42 °C. This trend is attributed to enhanced convective cooling, which promotes thermal dissipation from the panel surface.

These results align with thermal modelling predictions and highlight the role of airflow in maintaining lower operating temperatures and improving module longevity and efficiency. The inverse relationship observed between wind speed and cell temperature aligns with previous findings that identified wind-driven convective cooling as a key factor influencing photovoltaic efficiency [20, 21, 25, 36], as shown in Figure 8.

3.6. Validation of Predictive Efficiency Equation

Predicted PV efficiency was compared with measured values obtained from the Arduino-based monitoring system under different irradiance (200–1000 W/m²) and ambient temperature (15–40 °C) conditions. The results showed close agreement, with most deviations below 8%. This confirms that Equation (11) can represent PV efficiency under real operating conditions. Some small differences were observed during rapid changes in irradiance, which are expected due to sensor response time. A broader validation campaign across multiple seasons is planned for future work.

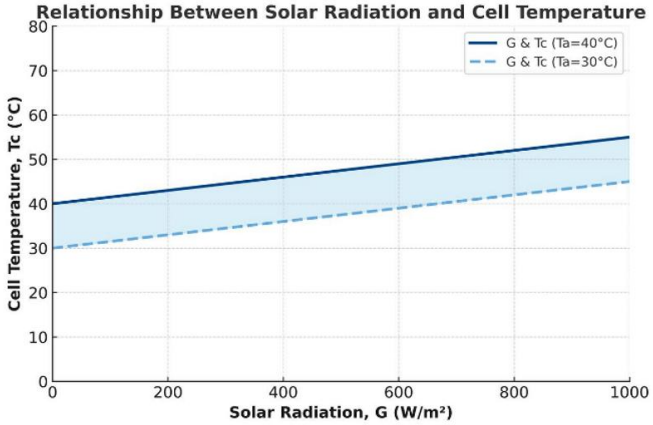

Fig. 7. Relationship between solar radiation and cell temperature.

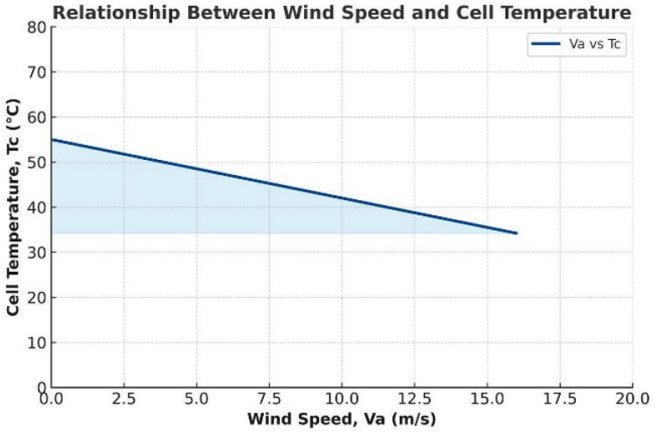

Fig. 8. Relationship between wind speed and cell temperature.

3.7. Seasonal Dynamics of Sunrise and Sunset Timing

Due to the Earth's axial tilt and orbital motion, sunrise and sunset times exhibit predictable seasonal shifts. Sunrise occurs as late as ~7:30 AM near the winter solstice and as early as ~5:00 AM near the summer solstice, while sunset ranges from ~4:45 PM in winter to ~7:30 PM in summer. This variation creates a seasonal daylight window difference of nearly four hours, which directly influences the amount of daily solar irradiance available for photovoltaic generation. Such fluctuations are critical for system sizing, seasonal energy yield forecasting, and determining the economic viability of fixed versus tracking PV installations. The symmetry of the pattern around the solstices also supports predictive scheduling for maintenance and grid integration. These implications are illustrated in Figure 9.

3.8. Integration of Environmental Measurements for Efficiency Prediction

The environmental parameters presented in Figures 4–9 are not independent observations but are directly incorporated into the predictive efficiency framework. Solar irradiance (G), ambient temperature (Ta), and wind speed (Va) are combined using Equation (9) to estimate cell temperature (Tc). In parallel, solar geometry parameters such as declination, hour angle, and incidence angle (θ) are computed from Equations (1–8). These values are then integrated into Equation (11) to calculate the total efficiency (Ƞ_Total). This process ensures that the measured variations in solar and meteorological factors are reflected in the efficiency predictions. To illustrate this integration, the predicted efficiency values were compared with experimental results obtained from the monitoring system, showing close agreement with deviations generally below 8%. This confirms that the combined use of Figures 4–9 provides a robust foundation for accurate efficiency prediction.

3.9. Comparative Discussion with Advanced PV Monitoring and Optimisation Systems

Recent approaches to PV performance prediction rely heavily on data-driven models (e.g., multiple linear regression and artificial neural networks) trained on historical weather and plant data [9], often producing accurate forecasts but typically operating offline and without embedded access to solar-geometry features. Thermal–electrical studies, in turn, provide strong physical fidelity for temperature and performance-ratio effects under varying environments [10], [16], [20], [21], while dedicated convection analyses quantify the cooling influence of wind over inclined modules [25], [26]. Field platforms demonstrate practical monitoring capability but are frequently tethered to external power, network infrastructure, or supervisory systems [29]. The present work is distinct in three ways.

First, it fuses astronomical modelling (declination, hour angle, incidence angle) with real-time measurements of irradiance, ambient/module temperature, and wind speed on a standalone, low-cost device, enabling site-specific assessment without external infrastructure.

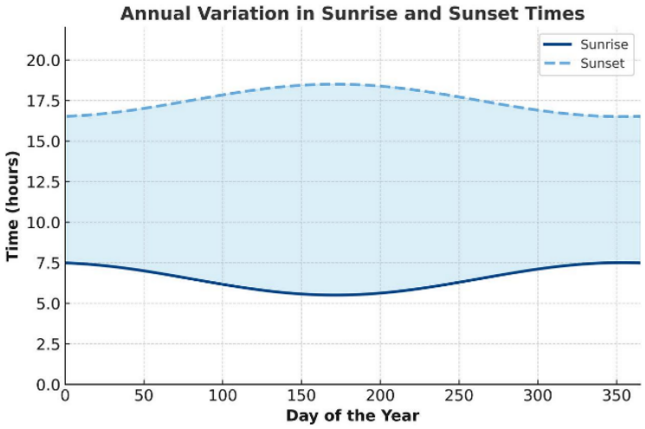

Fig. 9. Annual variation in sunrise and sunset times.

Second, the environmental variables are integrated explicitly: G, Ta, and Va feed a physical cell-temperature relation (Eq. 9), while the geometry-dependent incidence term links to the efficiency estimator (Eq. 11) that runs on-device. This closes the gap between offline physics and purely data-driven predictors by providing a transparent, physically modelling approach that can operate in the field.

Third, we include an experimental comparison between predicted and measured efficiency, demonstrating close agreement and supporting the model's practical utility.

Collectively, these features position the platform as a bridge between established monitoring systems and future optimisation workflows: the same feature set (geometry, irradiance, temperature, wind) is readily reusable for multivariate optimisation and machine-learning models, which we outline as the next phase of this research.

4. Conclusion

This investigation systematically examined the influence of environmental and astronomical variables on the thermal behaviour and energy conversion efficiency of photovoltaic (PV) systems across an annual cycle. The study established clear relationships between solar irradiance, ambient temperature, wind speed, and panel orientation by integrating continuous sensor-based measurements with computed solar geometry parameters. Elevated irradiance and ambient temperature were consistently associated with increased cell temperatures, whereas higher wind speeds provided effective convective cooling, mitigating thermal losses. Efficiency was also shown to be highly sensitive to the angle of incidence, highlighting the importance of dynamic orientation strategies in maximising energy yield.

These findings have practical implications for performance forecasting, site-specific panel placement, and targeted thermal management in real-world PV installations. Incorporating astronomical cycles—such as seasonal variations in day length and solar noon—into predictive models provides a more comprehensive framework for adaptive system design. Quantitatively, the system achieved an average efficiency of 13.02% (~87% of STC), while wind-driven cooling lowered cell temperatures by up to 12 °C and improved efficiency by ~2–3% under high irradiance. These

improvements demonstrate the practical performance gains achievable through integrated monitoring and modelling.

This study represents the first stage of a broader research agenda. Building on the integrated monitoring–modelling framework presented here, future work will apply multivariate analysis and machine learning techniques to the collected dataset. These approaches will enable predictive optimisation of PV orientation, cooling strategies, and installation parameters. Extended validation using industry-standard tools will further enhance the robustness of the proposed model.

Acknowledgements

The authors gratefully acknowledge the support of the Electrical Engineering Technical College staff for their invaluable support and assistance throughout this research. This study would not have been possible without their expert guidance and continuous encouragement. Their unwavering support has been instrumental in the successful completion of this work, and the authors sincerely appreciate their contributions.

References

[1] H. Rudchanka, N. Logacheva, and A. Uzhegov, "Global energy trends in the context of climate and environmental transformations," in E3S Web of Conferences, 2024, vol. 583: EDP Sciences, p. 08014.

[2] R. Newell, D. Raimi, S. Villanueva, and B. Prest, "Global energy outlook 2020: energy transition or energy addition," Resources for the Future, 2020.

[3] D. Raimi, E. Campbell, R. G. Newell, B. Prest, S. Villanueva, and J. Wingenroth, "Global energy outlook 2022: turning points and tension in the energy transition," Resources for the Future: Washington, DC, USA, 2022.

[4] A. O. Maka and T. N. Chaudhary, "Performance investigation of solar photovoltaic systems integrated with battery energy storage," Journal of Energy Storage, vol. 84, p. 110784, 2024.

[5] S. C. Obiora, O. Bamisile, Y. Hu, D. U. Ozsahin, and H. Adun, "Assessing the decarbonization of electricity generation in major emitting countries by 2030 and 2050: Transition to a high share renewable energy mix," Heliyon, vol. 10, no. 8, 2024.

[6] R. Ferroukhi, P. Frankl, and R. Adib, "Renewable energy policies in a time of transition: heating and cooling," 2020.

[7] T. Salamah, A. Ramahi, K. Alamara, A. Juaidi, R. Abdallah, M.A. Abdelkareem, E.C. Amer, and A.G. Olabi, "Effect of dust and methods of cleaning on the performance of solar PV module for different climate regions: Comprehensive review," Science of The Total Environment, vol. 827, p. 154050, 2022.

[8] G. Sahin, G. Isik, and W. G. van Sark, "Predictive modeling of PV solar power plant efficiency considering weather conditions: A comparative analysis of artificial neural networks and multiple linear regression," Energy Reports, vol. 10, pp. 2837-2849, 2023.

[9] B. Limane, C. Ould-Lahoucine, and S. Diaf, "Modeling and simulation of the thermal behavior and electrical performance of PV modules under different environment and operating conditions," Renewable Energy, vol. 219, p. 119420, 2023.

[10] L.D. Jathar, S. Ganesan, U. Awasarmol, K. Nikam, K. Shahapurkar, M. Elahi, M. Soudagar, H. Fayaz, A.S. El-Shafay, M.A. Kalam, S. Bouadila, S. Baddadi, V. Tirth, A.S. Nizami, S.S. Lam, and M. Rehan, "Comprehensive review of environmental factors influencing the performance of photovoltaic panels: Concern over emissions at various phases throughout the lifecycle," Environmental Pollution, vol. 326, p. 121474, 2023.

[11] M. R. Maghami, H. Hizam, C. Gomes, M. A. Radzi, M. I. Rezadad, and S. Hajighorbani, "Power loss due to soiling on solar panel: A review," Renewable and Sustainable Energy Reviews, vol. 59, pp. 1307-1316, 2016.

[12] M. F. Jaffar, A. T. Mohammad, and A. Q. Ahmed, "An experimental study for enhancing the performance of the photovoltaic module using forced air," Journal of Techniques, vol. 4, no. 2, pp. 1-9, 2022.

[13] C. Ramanan, K. H. Lim, J. C. Kurnia, S. Roy, B. J. Bora, and B. J. Medhi, "Design study on the parameters influencing the performance of floating solar PV," Renewable Energy, vol. 223, p. 120064, 2024.

[14] T. A. Kumar, C. S. Murthy, and A. Mangalpady, "Performance analysis of PV panel under varying surface temperature," in MATEC Web of Conferences, 2018, vol. 144: EDP Sciences, p. 04004.

[15] M. Dhimish, "Thermal impact on the performance ratio of photovoltaic systems: A case study of 8000 photovoltaic installations," Case Studies in Thermal Engineering, vol. 21, p. 100693, 2020.

[16] M. Mamun, M. Islam, M. Hasanuzzaman, and J. Selvaraj, "Effect of tilt angle on the performance and electrical parameters of a PV module: Comparative indoor and outdoor experimental investigation," Energy and Built Environment, vol. 3, no. 3, pp. 278-290, 2022.

[17] R. Conceição, H. G. Silva, L. Fialho, F. M. Lopes, and M. Collares-Pereira, "PV system design with the effect of soiling on the optimum tilt angle," Renewable Energy, vol. 133, pp. 787-796, 2019.

[18] E. Magadley, R. Kabha, and I. Yehia, "Outdoor comparison of two organic photovoltaic panels: The effect of solar incidence angles and incident irradiance," Renewable Energy, vol. 173, pp. 721-732, 2021.

[19] T. Huld and A. M. Gracia Amillo, "Estimating PV module performance over large geographical regions: The role of irradiance, air temperature, wind speed and solar spectrum," Energies, vol. 8, no. 6, pp. 5159-5181, 2015.

[20] L. Ghabuzyan, K. Pan, A. Fatahi, J. Kuo, and C. Baldus-Jeursen, "Thermal effects on photovoltaic array performance: Experimentation, modeling, and simulation," Applied Sciences, vol. 11, no. 4, p. 1460, 2021.

[21] A. K. Elfaqih, A. Elbaz, and M. A. Bashiri, "A Case Study on the Performance Degradation of a Photovoltaic System Module in Tripoli, Libya," International Journal of Renewable Energy Research (IJRER), vol. 15, no. 1, pp. 56-63, 2025.

[22] M. H. Ahmed, "Dynamic Simulation of the Annual Performance of PV-Wind System for Hydrogen Generation in Egypt Using TRNSYS," International Journal of Renewable Energy Research (IJRER), vol. 15, no. 1, pp. 77-86, 2025.

[23] S. Khemakhem and L. Krichen, "Local and Central Supervision of Optimal Plug-In Electric Vehicles Energy Dispatching for Load Smoothing within the Innovative Smart Grid," International Journal of Renewable Energy Research (IJRER), vol. 15, no. 1, pp. 96-107, 2025.

[24] Z. R. Tahir, A. Kanwal, M. Asim, M. Bilal, M. Abdullah, S. Saleem, M.A. Mujtaba, I. Veza, M. Mousa, and M.A. Kalam, "Effect of temperature and wind speed on efficiency of five photovoltaic module technologies for different climatic zones," Sustainability, vol. 14, no. 23, p. 15810, 2022.

[25] Y.-Y. Wu, S.-Y. Wu, and L. Xiao, "Numerical study on convection heat transfer from inclined PV panel under windy environment," Solar Energy, vol. 149, pp. 1-12, 2017.

[26] M. Usama, M. N. Qaiser, and H. A. Khan, "Solar irradiance, wind and temperature monitoring for residential PV applications," in 2015 IEEE 42nd Photovoltaic Specialist Conference (PVSC), 2015: IEEE, pp. 1-4.

[27] S. Mu, F. Ling, J. Wang, and I. Garip, "A Novel High-Gain Cuk-Sepic Converter with Coupled Inductor for Renewable Energy Applications," International Journal of Renewable Energy Research (IJRER), vol. 15, no. 1, pp. 152-160, 2025.

[28] H. Al-Saadi, A. J. Abid, and A. A. Obed, "Development and Field Evaluation of an Autonomous Solar Monitoring System for Enhanced Photovoltaic Performance," in 2025 13th International Conference on Smart Grid (icSmartGrid), 2025: IEEE, pp. 717-722.

[29] F. M. Al-Naima, R. S. Ali, and A. J. Abid, "Design of an embedded solar tracking system based on GPS and astronomical equations," International Journal of Information Technology and Web Engineering (IJITWE), vol. 9, no. 1, pp. 12-30, 2014.

[30] A. J. Abid and F. M. Al-Naima, "A Photovoltaic Measurement System for Performance Evaluation and Faults Detection at the Field," Int. J. Autom. Smart Technol, vol. 10, pp. 409-420, 2020.

[31] A. K. Abbas, A. A. Obed, and A. J. Abid, "Design of a Smart Energy Management System for Photovoltaic Stand-Alone Building," in IOP Conference Series: Materials Science and Engineering, 2020, vol. 881, no. 1: IOP Publishing, p. 012158.

[32] H. S. Ahmed, A. J. Abid, and A. A. Obed, "Mitigating Partial Shading Effects in Photovoltaic Arrays using a Switch Matrix: Design, Modeling, and Performance Evaluation," in 2023 Sixth International Conference on Vocational Education and Electrical Engineering (ICVEE), 2023: IEEE, pp. 202-208.

[33] L. Clavadetscher and T. Nordmann, "Cost and performance trends in grid-connected photovoltaic systems and case studies," Report IEA-PVPS T2-06, 2007.

[34] L. Clavadetscher, "Country reports on PV system performance. IEA-PVPS Task 2, activity 2.6," 2004.

[35] V. Ramasamy, J. Zuboy, M. Woodhouse, E. O'Shaughnessy, D. Feldman, J. Desai, A. Walker, R. Margolis, and P. Basore, "Us solar photovoltaic system and energy storage cost benchmarks, with minimum sustainable price analysis: Q1 2023," National Renewable Energy Laboratory (NREL), Golden, CO (United States), 2023.

[36] V. Rao, S. Kumar, J. Pothula, S. T. BV, and R. Vangalapudi, "Construct and Performance Investigation of a Hybrid ANFIS Controlled Islanded Micro-Grid," International Journal of Renewable Energy Research (IJRER), vol. 15, no. 1, pp. 161-171, 2025.